



## Structure and dynamics behaviors of pinostrobin binding inside cyclodextrin cavity

Jintawee Kicuntod<sup>1</sup>, Wasinee khuntawee<sup>2</sup>, Peter Wolschann<sup>3,4</sup>, Piamsook Pongsawasdi<sup>1</sup>, Thanyada Rungrotmongkol<sup>1,\*</sup>

<sup>1</sup>Department of Biochemistry, Faculty of Science, Chulalongkorn University, Thailand

<sup>2</sup>Nanoscience and Technology Program, Graduate School, Chulalongkorn University, Thailand

<sup>3</sup>Institute for Theoretical Chemistry, University of Vienna, Austria

<sup>4</sup>Department of Pharmaceutical Technology and Biopharmaceutics, University of Vienna, Austria

\*e-mail: t.rungrotmongkol@gmail.com, thanyada.r@chula.ac.th

### Abstract

Pinostrobin (PNS) is one of the most important flavonoids which exhibit many biological activities such as anti-oxidation, anti-inflammatory and anti-cancer. Unfortunately, it has an extremely low water solubility leading to a limitation in the pharmaceutical applications. In general, cyclodextrins (CDs) are able to enhance the solubility and stability of the poorly soluble compound by encapsulation process. Here, the structure and dynamics properties of complexation of pinostrobin and  $\beta$ -CD as well as its derivative 2,6-dimethyl  $\beta$ -cyclodextrin (DM- $\beta$ -CD) were studied by the computational methods, molecular docking and molecular dynamics simulations. As a result, there were two possible forms of inclusion complexes, the chromone or phenyl ring of pinostrobin inserted into the CD cavity, called C-PNS/CD and P-PNS/CD. C-PNS molecule stably occupied within the CD cavity is likely better than that of P-PNS. More solvations around the oxygen atoms of the pinostrobin were observed in the P-PNS/CD complexes because the phenyl ring positioned on the wider rim exposed to water accessibility.

**Keywords:** Pinostrobin, flavonoids, cyclodextrins, molecular dynamics simulation

### Introduction

Flavonoids are a large family of polyphenolic compounds synthesized by plants (Beecher, 2003). These compounds are abundant in fruits, vegetables and herbs (Formica and Regelson, 1995). Flavonoids exhibit a multitude of biological properties, such as anti-bacteria, anti-allergy and anti-oxidation (Hollman and Katan, 1997), (Rice-Evans et al., 1996). Due to their pharmacological potential and nutritional effects, the flavonoids are considerable interests for drug as well as health food supplement. Pinostrobin (PNS, structure in Figure 1A.) belongs to the flavanone subclass of flavonoids which is mostly found in Thai galingale and rhizome of *Boesenbergia rotunda*. It has multiple biological activities such as anti-inflammatory role cyclooxygenase (COX) enzyme (O'Leary et al., 2004), anti-aromatase (Le bail et al., 2000), decreased growth rate of a breast cancer cell line (MCF-7) (Le bail et al., 2000) and inhibition of HIV-1 protease (HIV-PR) (Tewtrakul et al., 2003). However, pharmacological limitation of pinostrobin has been reported because it has very poor water solubility. Cyclodextrin (CD) is a cyclic oligosaccharide (Tiwari et al., 2010) comprising D-(+)-glucopyranose units linked through  $\alpha$ -1,4 glycosidic bonds as shown in Figure 1B. It has the torus shape with hydrophilic outer surface and relatively hydrophobic cavity. The solubility of poorly soluble compounds can be improved by insertion of their hydrophobic motif inside the CD's cavity (Radi and Eissa, 2010). Naturally, the CDs contain six, seven and eight glucopyranoside units are known as  $\alpha$ -CD,  $\beta$ -CD, and  $\gamma$ -CD, respectively. The regular  $\beta$ -CD is commercially used because of high yield synthesis and low cost. Since the  $\beta$ -CD shows the lowest solubility

among the three types of CD, its derivatives, for example 2,6-dimethyl  $\beta$ -cyclodextrin (DM- $\beta$ -CD) with > 25-fold increased solubility relative to  $\beta$ -CD, are frequently used in the applications. In the recent years, the computational approaches have been played an important role for monitoring inclusion complex between cyclodextrins and guest molecules including flavonoids in molecular level (Zhang et al., 2010). In case of quercetin and myricetin in a group of flavonoids, the molecular dynamics (MD) simulations were used to describe the formed inclusion complex in comparison to the experimental results from  $^1\text{H}$ -NMR spectroscopy (Zheng et al., 2008). By MD simulations, Sangpheak and co-authors (Sangpheak et al., 2014) has reported a higher stability of naringenin complex with the DM- $\beta$ -CD in respect to  $\beta$ -CD. Therefore in the present study, the MD simulations were used to obtain the molecular details of structural and dynamical properties of pinostrobin in complex with  $\beta$ -CD and its dimethyl derivative, DM- $\beta$ -CD (PNS/ $\beta$ -CD and PNS/DM- $\beta$ -CD). The binding mode and orientation, stability and solvation of pinostrobin in the inclusion complex were considered and discussed.

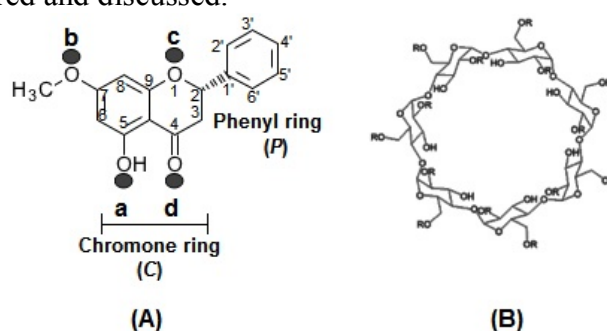


**Figure 1** Two dimensional structures of (A) pinostrobin and (B)  $\beta$ -cyclodextrin and its dimethyl derivative DM- $\beta$ -CD where -R is -H and -CH<sub>3</sub>, respectively. The labeled atomic names and four interaction sites (a-d) of pinostrobin are defined in according to their oxygen atoms for further discussion.

## Methodology

The starting conformation of pinostrobin was fully optimized by the *ab initio* calculation using HF/6-31\* basis set in Gaussian09 program (Alecú et al., 2010) while the optimized structures of  $\beta$ -CD and DM- $\beta$ -CD were taken from our previous works (Snor et al., 2007). Prediction of a pinostrobin in inclusion complex with  $\beta$ -CD and DM- $\beta$ -CD was performed by docking procedure with 500 independent runs using the CDocker module of Accelrys Discovery Studio 2.5 [Accelrys, Inc.]. The docked inclusion complex with the best ranked interaction energy and the highest number hydrogen bond formation between pinostrobin and cyclodextrins was chosen for the molecular dynamics study. The following system preparation and MD simulation on the focused inclusion complexes were performed with the Amber 12 software package (Walker R.C. et al., 2008). The Glycam-06 bimolecular force field (Kirschner et al., 2008) was applied for the cyclodextrins. In case of pinostrobin, the atomic charges and parameters were developed in according to the standard procedures (Khuntawee et al., 2012 and Kaiyawet et al., 2013). The electrostatic potential (ESP) charges around the optimized molecule of pinostrobin was evaluated by the same method and basis set above using Gaussian09. Its restrained electrostatic potential (RESP) charges were then obtained by charge fitting procedure using the antechamber module implemented in Amber 12 was applied. The hydrogen atoms of the inclusion complex were minimized with the 1000 steps of steepest descents (SD) followed by the 3000 steps of conjugated gradients (CG) to relax structure and release bad contact. The complex was consequently solvated by the SPC water molecules with spacing distance of 12 Å around the surface of inclusion complex. Each

system consisted of  $1,400 \pm 42$  water molecules in the  $45 \times 45 \times 45 \text{ \AA}^3$  truncated octahedron periodic box. The water molecules were only minimized with the SD (1000 steps) and CG (3000 steps), and then the whole system was minimized with the same process. In the next step, the MD simulation with periodic boundary condition using *NPT* ensemble and time step of 2 fs was performed. The electrostatic interactions were taken into account by the particle mesh Ewald approach (Luty et al., 1996) with a cutoff distance of  $12 \text{ \AA}$ . The SHAKE algorithm was used to constrain all bonds involving hydrogen atoms. The systems were heated up to 298 K with the relaxation time of 100 ps and then simulated at the same temperature for 20 ns. The MD trajectories were recorded every 500 steps for analysis. The root means square displacement (RMSD), pinostrobin conformation, distance between centers of gravity of pinostrobin and cyclodextrin, and the radial distribution function (RDF) of waters around the oxygen atoms of pinostrobin were analyzed by the ptraj module.

## Results and Discussion

### Binding mode of pinostrobin

The percentage of occurrences, interaction energy and hydrogen bond (H-bond) formation of pinostrobin inside the hydrophobic cavity of cyclodextrin resulted from docking calculation are given in Table 1. Based on interaction energy and H-bond formation between pinostrobin and cyclodextrin, the best formed inclusion complexes with  $\beta$ -CD and DM- $\beta$ -CD are depicted in Figure 2. From the 500 independent docking runs, the two different binding modes of pinostrobin in the cavity of  $\beta$ -CD and DM- $\beta$ -CD were observed. For *C*-PNS/ $\beta$ -CD and *C*-PNS/DM- $\beta$ -CD (Figures 2A and 2C), the chromone ring of pinostrobin was located inside the cyclodextrin cavity close to the primary rim, whereas for *P*-PNS/ $\beta$ -CD and *P*-PNS/DM- $\beta$ -CD (Figures 2B and 2D), its phenyl ring was inserted instead. It can be seen that pinostrobin's chromone ring preferred to dip inside  $\beta$ -CD and DM- $\beta$ -CD cavity with 79% and 68% of occurrences, respectively. Interestingly, the hydrogen bond was only detected in *P*-PNS/ $\beta$ -CD inclusion complex between hydroxyl group of PNS's chromone ring and the hydroxyl group at the O3 position on the secondary rim of CD ( $2.16 \text{ \AA}$ ). This may lead to a more stability of *P*-PNS/ $\beta$ -CD complex than *C*-PNS/ $\beta$ -CD complex in gas phase as observed by interaction energy of  $-26.28 \text{ kcal/mol}$  and  $-25.25 \text{ kcal/mol}$ , respectively. To further study on dynamics behaviors of PNS/CD inclusion complexes with different binding modes in aqueous solution, the MD simulations were applied on these four docked complexes (*C*-PNS/ $\beta$ -CD, *P*-PNS/ $\beta$ -CD, *C*-PNS/DM- $\beta$ -CD and *P*-PNS/DM- $\beta$ -CD).

**Table 1** Percentage of possible formed inclusion complex together with the interaction energy (kcal/mol) and number of H-bond formation of pinostrobin in the interior of  $\beta$ -CD and DM- $\beta$ -CD cavity for the best docked complex

complex	%docked conformation	Interaction energy (kcal/mol)	H-bond (distance, $\text{\AA}$ )
<i>C</i> -PNS/ $\beta$ -CD	79	-25.25	-
<i>P</i> -PNS/ $\beta$ -CD	21	-26.28	2.16
<i>C</i> -PNS/DM- $\beta$ -CD	68	-24.42	-
<i>P</i> -PNS/DM- $\beta$ -CD	32	-29.24	-

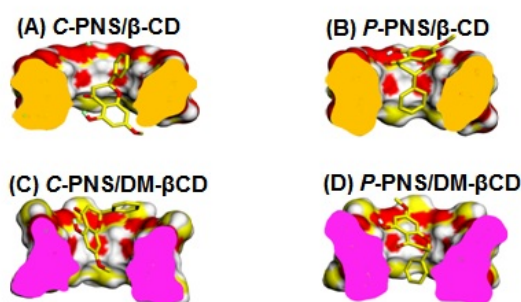


**Figure 2** Cutaway view of CD hydrophobic cavity showing (A and C) chromone ring and (B and D) phenyl ring of pinostrobin inserted in the cavity of two focused cyclodextrins,  $\beta$ -CD and DM- $\beta$ -CD

### Stability of simulated system

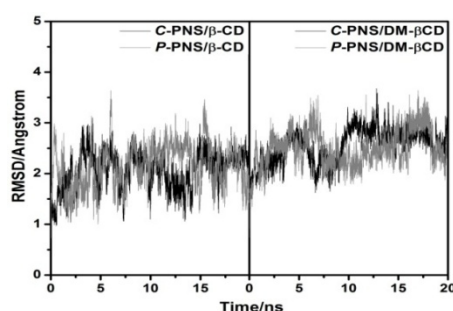


**Figure 3** RMSD plots of all atoms for the simulated systems of pinostrobin in complex with  $\beta$ -CD and DM- $\beta$ -CD in two different binding modes along the simulation time

The system stability of each inclusion complex in solution was monitored using the RMSD calculation. Figure 3 shows the RMSD plots for all atoms of inclusion complexes between cyclodextrin and pinostrobin with chromone ring (black) and phenyl ring (gray) dipping into the cavity and locating close to the primary rim. It can be described that all simulated systems had reached equilibrium at 10 ns, and so the MD trajectories from the last 10 ns of each simulation were used for further analysis, in particular the water accessibility towards pinostrobin in the formed inclusion complex in the last section.

### Conformational change of pinostrobin

To investigate the ligand conformational change inside the hydrophobic cavity of  $\beta$ -CD and DM- $\beta$ -CD, two structural parameters, C4'...C6 distance and O1...C2...C1'...C6' torsional angle (defined atom names in Figure 1A) of pinostrobin, *versus* the simulation time were measured and plotted in Figure 4. In C-PNS/ $\beta$ -CD complex (Figure 4A), the C4'...C6 distance continuously decreased from  $\sim 4$  Å to  $\sim 2$  Å and the highly fluctuated O1...C2...C1'...C6' torsional angle within the first 10 ns suggesting the chromone and phenyl rings of PNS were orientated to be closer to each other. The similar orientation of PNS was found in the C-PNS/DM- $\beta$ -CD complex (Figure 4C), however its preferential torsion ( $50^\circ$ ) was in the opposite site ( $-50^\circ$  for C-PNS/ $\beta$ -CD). Differentially, these two rings of PNS in both P-PNS/CD complexes (Figures 4B and 4D) likely moved apart from each other ( $\sim 5$ -6 Å), and then its torsion between the rings can rotate rather freely.

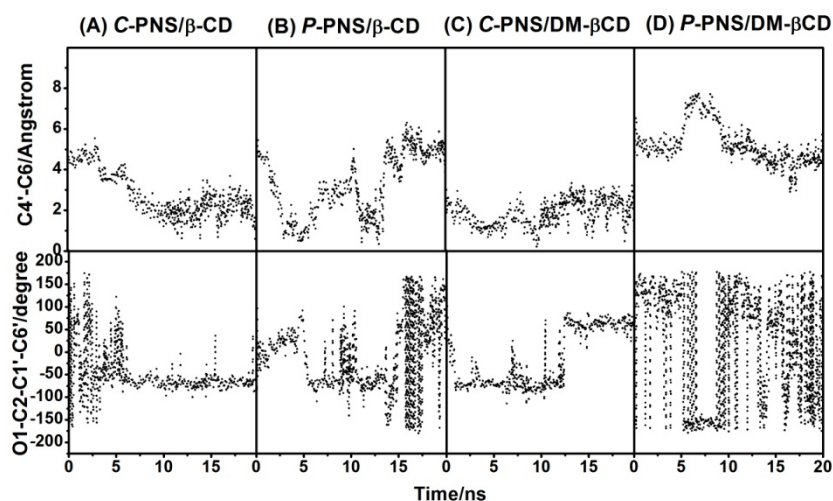


**Figure 4** Conformational change of pinostrobin in terms of distance ( $C4' \cdots C6$ ) and torsion angle ( $O1 \cdots C2 \cdots C1' \cdots C6'$ ) as a function of time for (A)  $C$ -PNS/ $\beta$ -CD, (B)  $P$ -PNS/ $\beta$ -CD, (C)  $C$ -PNS/DM- $\beta$ -CD and (D)  $P$ -PNS/DM- $\beta$ -CD

#### Ligand binding mode and mobility

To determine the dynamics behavior of pinostrobin molecule binding in the interior of the cyclodextrin, the distance between the center of gravity of pinostrobin,  $Cg(C/P$ -PNS), and the center of gravity of cyclodextrin,  $Cg(CD)$ , was measured along simulation time. The results for the four focused systems were plotted and compared in Figure 5, where the horizontal dash lines at  $-3.95 \text{ \AA}$  to  $3.95 \text{ \AA}$  represented the  $\beta$ -CD height of  $7.9 \text{ \AA}$  as reported in the previous study (Yang et al., 2013). Note that the height of DM- $\beta$ -CD cavity is  $10 \text{ \AA}$ . (Bekers et al., 1991). From Figure 5A, the distance between  $C$ -PNS and  $\beta$ -CD (black) increased from  $\sim 2 \text{ \AA}$  to  $\sim 1 \text{ \AA}$  at 5ns till the end of simulation showed that the  $C$ -PNS likely stayed and binding at the  $\beta$ -CD's center. In contrast, the higher mobility of PNS within the cavity of  $\beta$ -CD was observed in the  $P$ -PNS/ $\beta$ -CD complex (gray) in which the PNS was able to move from one end to the other end of cavity. For PNS/DM- $\beta$ -CD complex (Figure 5B), the distance between  $C$ -PNS and DM- $\beta$ -CD was mostly kept at  $\sim 1 \text{ \AA}$  along the simulation time implying that  $C$ -PNS was well occupied inside the DM- $\beta$ -CD hydrophobic cavity. The  $P$ -PNS was somewhat moved outside the secondary rim of DM- $\beta$ -CD during 5-10 ns and then moved back to stay within the cavity near the secondary rim. Therefore, it can be presumed that the  $C$ -PNS molecule was significantly better fitted in both CD cavities than  $P$ -PNS.

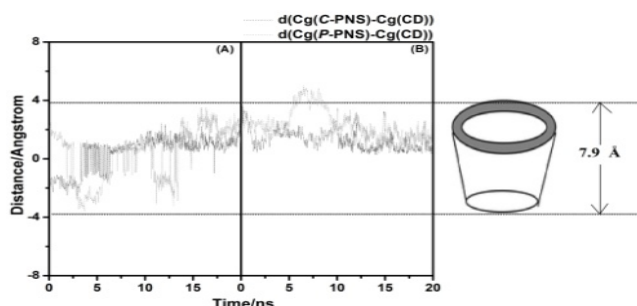


**Figure 5** Distance between the center of gravity of PNS,  $Cg(C/P$ -PNS), and center of gravity of cyclodextrin,  $Cg(CD)$ , for (A) PNS/ $\beta$ -CD complex and (B) PNS/DM- $\beta$ -CD complex. Dash lines represent the  $\beta$ -CD cavity height.

#### Water accessibility to pinostrobin

To gain the information of the water distribution around the oxygen atoms of pinostrobin molecule at the four sites (a-d in Figure 1A), the radial distribution functions (RDFs) of water oxygen atoms around each focused site were plotted together with integration number  $n(r)$  in Figure 6 for PNS/ $\beta$ -CD and PNS/DM- $\beta$ -CD complexes in both forms *C*-PNS (black) and *P*-PNS (gray). The water accessibility towards these four sites was estimated from the  $n(r)$  value determined at the first minima. Among the four sites of PNS/ $\beta$ -CD and PNS/DM- $\beta$ -CD complexes, only the c-site had no sharp peak of hydration shell suggesting that this site of compound had rather weak interaction with water probably due to this oxygen being as a member atom in the chromone ring and always staying inside the center of CD hydrophobic cavity. On the other hand, the other sites show the first sharp peak approximately at  $\sim 3$  Å corresponding to plentifully possible hydration and the first minima peak at  $\sim 4$  Å accounting for the distance when a water molecule sustain on the first hydration shell. At these three sites, waters can be more accessible to solvate the oxygen atoms of *P*-PNS than *C*-PNS in particular at the a- and b-sites because the chromone ring of *P*-PNS stayed nearby the secondary rim of CDs. No water molecule was trapped in the inclusion complex as seen by all minima locating above the  $g(r)$  of 0.0. Furthermore, the RDF plots could reveal that the water interactions of PNS/ $\beta$ -CD and PNS/DM- $\beta$ -CD complexes were qualitatively similar, and the increased solubility of PNS/DM- $\beta$ -CD complex over PNS/ $\beta$ -CD might be suggested by the higher total water solvation of PNS/DM- $\beta$ -CD (7.7 and 11.0 waters for *C*-PNS and *P*-PNS) than the complex of  $\beta$ -CD (6.8 and 10.8 waters).

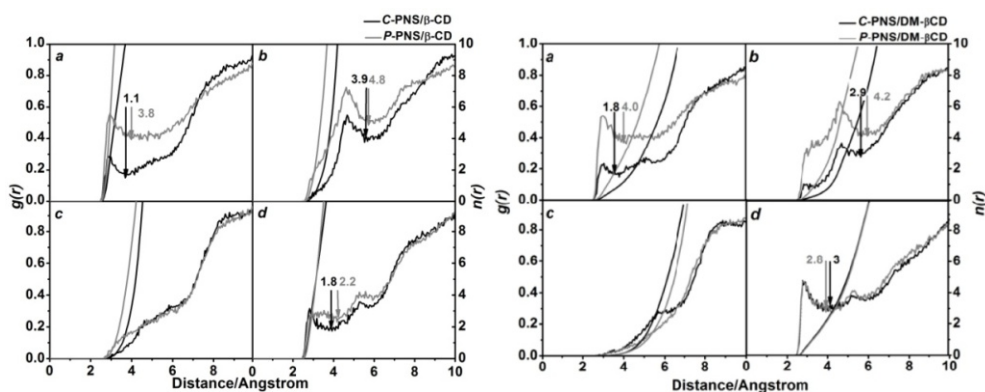


**Figure 6** Radial distribution function (RDF) of waters around the oxygen atoms at the a-d sites (defined in Figure 1A) for PNS/ $\beta$ -CD (left) and PNS/DM- $\beta$ -CD complexes (right) with the chromone (black) or phenyl (gray) ring binding in the cavity interior

## Conclusions

In the present work, the structural properties, dynamical properties, binding interaction and solvation effect of inclusion complexes of pinostrobin, guest molecule, with the  $\beta$ -CD and DM- $\beta$ -CD, host molecules, were investigated by the molecular docking and classical molecular dynamic simulations. By means of molecular docking, there are two possible forms of inclusion complex, the chromone ring (*C*-PNS) and phenyl ring (*P*-PNS) insertion into the cavity of both regular  $\beta$ -CD and DM- $\beta$ -CD. The pinostrobin prefers to insert inside the CD's cavity with through chromone ring more than phenyl ring. Moreover, the both rings of DM- $\beta$ -CD complex were well interacted with solvated water molecules that leading to have more water solubility than regular  $\beta$ -CD.

## Acknowledgements

This study was supported by the Scholarship from Graduated School, Chulalongkorn University to commemorate the 72<sup>nd</sup> anniversary of his Majesty King Bhumibala Aduladeja. TR thanks the TRF-CHE Research Grant for New Scholars (MRG5580223). The Computer Chemistry Unit Cell, and the Vienna Scientific Cluster (VSC-2) are acknowledged for facility and computing resources.

## References

- Alecu I., Zheng J., Zhao Y. and Truhlar D.G. (2010) Computational Thermochemistry: Scale factor database and scale factors of vibrational frequencies obtained from electronic model chemistries. *J Chem Theory Comput* 6: 2872-2887.
- Beecher GR. (2003) Overview of dietary flavonoids: nomenclature, occurrence and intake. *J Nutr* 10: 3248S-3254S.
- Beker O., Uijtendaal E.V., Beijnen J.H., Bult A. and Underberg W.J.M. (1991) Cyclodextrins in the pharmaceutical field. *J Drug Dev Ind Pharm* 17: 1503-1549.
- Formica JV. and Regelson W. (1995) Review of the biology of quercetin and related bioflavonoids. *J Food Chem Toxicol* 33: 1061-1080.
- Hollman P.C.H. and Katan M.B. (1997) Absorption, metabolism, and health effects of dietary flavonoids in man. *J Biomed Pharmacother* 51: 305-310.
- Kaiyawet N., Rungrotmongkol T. and Hannongbua S. (2013) Effect of halogen substitutions on dUMP to stability of thymidylate synthase/dUMP/mTHF ternary complex using molecular dynamics simulation. *J Chem Inf Model* 6: 1315-1323.
- Khuntawee W., Rungrotmongkol T., Hannongbua. (2012) Molecular dynamic behavior and binding affinity of flavonoid analogues to the cyclin dependent Kinase 6/cyclin D complex. *J Chem Inf Mol* 52: 76-83.
- Kirschner K.N., Yongye A.B., Tschampel S.M., Gonzalez-Outeirino J., Daniels C.R., Foley B.L. and Woods R.J. (2008) GLYCAM06: A generalizable biomolecular force field Carbohydrates. *J Comp Chem* 29: 622-655.
- Le Bail J.C., Aubourg L. and Habrioux G. (2000) Effects of pinostrobin on estrogen metabolism and estrogen receptor transactivation. *Lett Cancer* 156: 37-44.
- Luty B.A. and Gunsteren W.F. (1996) Calculating electrostatic interactions using the particle-particle particle-mesh method with nonperiodic long-range interactions. *J Phys Chem* 100: 2581-2587.
- O'Leary KA., Pascual-Tereasa S., Needs P.W., Bao Y.P., O'Brien N.M. and Williamson G. (2004) Effect of flavonoids and vitamin E on cyclooxygenase-2 (COX-2) transcription. *J Mutat Res* 551: 245-254.
- Radi AE. And Eissa S. (2010) Electrochemistry of cyclodextrin inclusion complexes of pharmaceutical compounds. *J Open Chem Biomed Meth* 3:74-85
- Rice-Evans C.A., Miller N.J. and Paganga G. (1996) Structure-antioxidant activity relationships of flavonoids and phenolic acids. *J Free Radic* 20: 933-956.
- Sangpheak W., Khuntawee W., Wolschann P., Pongsawasdi P., Rungrotmongkol T. (2014) Enhanced stability of a naringenin/2,6-dimethyl  $\beta$ -cyclodextrin inclusion complex: Molecular dynamics and free energy calculations based on MM- and QM-PBSA/GBSA. *J Mol Graph Model* 50: 10-15.
- Snor W., Liedl E., Weiss-Greiler P., Karpfen A., Viernstein H., Wolschann P. (2007) On the structure of anhydrous  $\beta$ -cyclodextrin. *Lett Chem Phys* 441: 159-162.
- Tewtrakul S., Subhadhirasakul S., Puripattanavong J. and Panphadung T. (2003) HIV-1 protease inhibitory substances from rhizomes of *Boesenbergia pandurata* Holtt. *Songklanakarinn J Sci Technol* 25: 503-508.
- Tiwari Gaurav, Tiwari Ruchi and Rai Awani K. (2010) Cyclodextrins in delivery systems: Applications. *J Pharm Bioallied Sci* 2: 72-79.

Walker R.C., Crowley M.F. and Case D.A. (2008) The Implementation of a fast and accurate QM/MM potential method in AMBER. *J Comp Chem* 29:1019-1031.

Yang L.-J., Ma S.-X., Zhou S.-Y., Chen W., Yuan M.-W., Yin Y.-Q. and Yang X.-D. (2013) Preparation and characterization of inclusion complexes of naringenin with  $\beta$ -cyclodextrin or its derivative. *J Carbohydr Polym* 98: 861-869.

Zhang H., Feng W., Li C. and Tan T. (2010) Investigation of the inclusions of puerarin and daidzin with  $\beta$ -cyclodextrin by molecular dynamics simulation. *J Phys Chem* 114: 4876–4883.

Zheng Y., Chow, Albert H.L., Haworth and Ian S. (2008) Molecular modeling of flavonoid- $\beta$ -cyclodextrin complexes. *Lett Drug Des Discov* 5:512-520.